Instantaneous phase-angle estimation algorithm under unbalanced voltage-sag conditions

H.-S.Song and K.Nam

Abstract: If a negative sequence is generated by voltage sag and/or unbalance, it appears as an oscillating error in a synchronous reference frame (SRF). In power conditioning equipment, the exact value of a positive sequence is needed to achieve the unity power factor and constant output voltage, whereas the exact value of a negative sequence is needed for unbalance compensation. To measure the positive sequence separately from the negative sequence, a low pass or notch filter having a narrow bandwidth is normally used. However, such a filter causes a lot of phase delay, thus the response time of the system tends to be lengthened. A method of estimating the positive- and the negative-sequence voltages separately is presented, without a significant delay, by utilising the weighted least-squares estimation (WLSE) method with the covariance resetting technique. A frequency update law is also proposed to accommodate the frequency varying environments. The authors demonstrate through simulation and experiment the superior performance of the proposed scheme in measuring the positive- and the negative-sequence voltages at the time of abrupt transition. This method can be applied to uninterruptable power supplies (UPS), pulsewidth modulation (PWM) AC/DC converters, active filters, AC voltage compensators etc.

Nomenclature

E_a, E_b, E_c	= Three-phase source voltage, V
$\boldsymbol{E}_{dqs}$ $(= E_{ds} + jE_{qs})$	= Voltage vector having d- and q-axis voltage in the stationary frame
$\boldsymbol{E}^p_{dqe}$ $(= E^p_{de} + jE^p_{qe})$	= Positive-sequence voltage vector in its synchronous reference frame
$\boldsymbol{E}^n_{dqe}$ $(= E^n_{de} + jE^n_{qe})$	= Negative-sequence voltage vector in its synchronous reference frame
superscript p	= Positive-sequence component
superscript n	= Negative-sequence component
subscript s	= Quantity in the stationary frame
subscript e	= Quantity in the synchronous reference frame
subscript d	= Direct-axis quantity
subscript q	= Quadrature-axis quantity
SRF	= Synchronous reference frame
WLSE	= Weighted least-squares estimation
ω	= Source frequency, rad/s
φ	= Phase angle of the source voltage, rad
ϕ	= Phase angle of the positive-sequence voltage in the SRF, rad
$\tilde{\phi}$	= Phase error caused by the negative sequence, rad

IEE Proceedings online no. 20000716

DOI: 10.1049/ip-gtd:20000716

Paper first received 10th January and in revised form 11th July 2000

The authors are with the Department of Electrical Engineering, POSTECH University, Hyoja San-31, Pohang, 790-784 Republic of Korea

1 Introduction

The phase angle of a source voltage is used to calculate and control the flow of active/reactive power, and transform the feedback variables to a synchronous reference frame (SRF) [1, 2]. The phase angle, therefore, is a critical piece of information for the operation of most power-conditioning equipment, such as pulsewidth modulation (PWM) AC/DC converter, uninterruptable power supplies (UPS), AC voltage compensators, static VAR compensators (SVC), active harmonic filters etc. If a voltage sag takes place in one or two phases in a three-phase power system, it causes an unbalance by generating a negative-sequence voltage. As the voltage vector of an unbalanced three-phase voltage is expressed as a sum of positive- and negative-sequence components, it is hard to find the SRF that is tuned only to the positive-sequence component. Note that the vector of a negative-sequence component, rotating in the opposite direction, looks like a 120Hz oscillating ripple in the SRF of a 60Hz system [3, 4]. Obviously, the positive-sequence component appears as DC in the SRF. In the power conditioning equipment, both the positive- and the negative-sequence components should be measured correctly. Otherwise, it may not compensate voltage properly, and thus cause the performance to deteriorate.

To separate the DC component from 120 Hz ripple caused by the unbalance, Hochgraf and Lasseter [5] used a notch filter. However, the use of a filter typically generates phase delay and results in a sluggish response, and causes some time-critical machines to malfunction.

Sidhu and Sachdev [6] presented an iterative technique for estimating frequency and phase. However, as their method requires a great deal of computational effort, it does not seem to be appropriate for the control of UPS or PWM converter.

In this work, the authors propose an instantaneous phase-angle estimation algorithm that operates well, even

under sudden voltage sag and/or unbalance conditions, and a frequency update law to accommodate a frequency-varying environment. The algorithm is derived from the weighted least-squares estimation (WLSE) method having the covariance resetting technique. With the proposed estimation method, the positive- and negative-sequence voltages can be found separately, almost without a significant delay.

2 Effects of a voltage unbalance on phase measurement

An unbalanced three-phase source voltage $\{E_a, E_b, E_c\}$ without a zero sequence can be represented as the orthogonal sum of the positive and negative sequences, such that [3]

$$\boldsymbol{E}_{dqs}(t_i) = e^{j\omega t_i}\boldsymbol{E}^p_{dqe}(t_i) + e^{-j\omega t_i}\boldsymbol{E}^n_{dqe}(t_i) \quad (1)$$

where $\boldsymbol{E}_{dqs} = \frac{2}{3}[E_a + E_b e^{j2\pi/3} + E_c e^{j2\pi/3}]$, $\boldsymbol{E}^p_{dqe} = E^p_{de} + jE^p_{qe}$, $\boldsymbol{E}^n_{dqe} = E^n_{de} + jE^n_{qe}$, $\omega = 2\pi \times 60$ [rad/s] is the source frequency. The subscripts s and e denote the quantities in the stationary frame and in the SRF of ωt_i, respectively. The superscripts p and n denote the quantities of positive and negative sequences, respectively. As the zero sequence has nothing to do with the phase angle, the authors just assume that there is no zero sequence. Multiplying $e^{j\omega t i}$ to eqn. 1, the authors measure the phase angle defined by

$$\begin{aligned}\varphi(t_i) &= \angle(-e^{j\omega t_i}\boldsymbol{E}_{dqs}(t_i)),\\ &= \angle(\boldsymbol{E}^p_{dqe}(t_i) + e^{-2j\omega t_i}\boldsymbol{E}^n_{dqe}(t_i)),\\ &= \phi(t_i) + \tilde{\phi}(t_i)\end{aligned} \quad (2)$$

where $\phi(t_i) \equiv \angle\boldsymbol{E}^p_{dqe}(t_i)$ denotes the phase angle of the positive-sequence voltage in the SRF of ωt_i and $\tilde{\phi}(t_i) \equiv \varphi(t_i) - \angle\boldsymbol{E}^p_{dqe}(t_i)$ denotes the oscillatory phase error caused by the negative sequence. Fig. 1 shows the relationship among $\phi(t_i)$, $\tilde{\phi}(t_i)$, and $\varphi(t_i)$. Under the normal balanced three-phase voltage condition, $\varphi(t_i) = \phi(t_i)$ and $\tilde{\phi}(t_i) = 0$, i.e. $\varphi(t_i)$ contains only a DC component. However, under unbalanced voltage-sag conditions, $\tilde{\phi}(t_i)$ comprises 120Hz AC ripple.

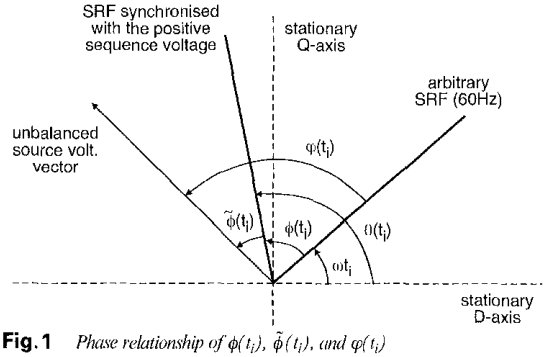

Fig. 1 *Phase relationship of $\phi(t_i)$, $\tilde{\phi}(t_i)$, and $\varphi(t_i)$*

Fig. 2 shows the effect of the unbalanced voltage on the phase angle measurement. Fig. 2*a* shows the three-phase source voltage $\{E_a, E_b, E_c\}$ and $\varphi(t_i)$, when a balanced three-phase voltage is applied. On the other hand, Fig. 2*b* shows the same components, when a three-phase voltage is unbalanced. It can be clearly seen from Fig. 2*b* that the negative-sequence voltage $\boldsymbol{E}^n_{dqe}$ resulting from the voltage unbalance causes a 120Hz oscillating error $\tilde{\phi}(t_i)$ in the phase-angle measurement.

For the complete compensation of voltage sag and/or unbalance, it is necessary to identify $\phi(t_i)$. In the process of measuring $\phi(t_i)$ by using a conventional PLL or a lowpass (or notch) filter, an inherent problem will be confronted, namely the phase delay. A notch filter is known to be more effective in reducing the phase delay [5, 7, 8]. Nevertheless, with the conventional method, a few cycles are often lost before proper compensation action starts. In some time-critical machines, such as voltage compensators or UPS, the phase delay sometimes limits their applications.

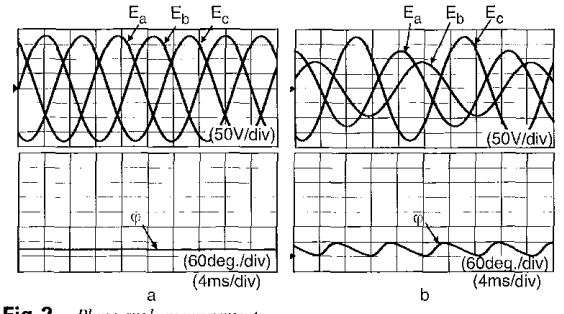

Fig. 2 *Phase-angle measurements*
a Source voltage is balanced
b Source voltage is unbalanced

3 Principles of an instantaneous phase-angle estimation algorithm

In this Section, a phase-angle estimation algorithm is developed from positive-sequence voltage with the use of the weighted least-squares estimation (WLSE) method. Also, a frequency update algorithm is proposed to track the source frequency when it is varying.

3.1 Weighted least-squares estimation algorithm for the phase-angle estimation

Expressing eqn. 1 in the matrix form, the following is obtained:

$$\boldsymbol{y}(t_i) = \boldsymbol{H}(t_i)\boldsymbol{x}(t_i) \quad (3)$$

where

$$\boldsymbol{H}(t_i) \equiv \begin{bmatrix}\cos(\omega t_i) & -\sin(\omega t_i) & \cos(\omega t_i) & \sin(\omega t_i)\\ \sin(\omega t_i) & \cos(\omega t_i) & -\sin(\omega t_i) & \cos(\omega t_i)\end{bmatrix} \quad (4)$$

$$\boldsymbol{x}(t_i) \equiv \left[E^p_{de}(t_i)\ E^p_{qe}(t_i)\ E^n_{de}(t_i)\ E^n_{qe}(t_i)\right]^T \quad (5)$$

$$\boldsymbol{y}(t_i) \equiv \begin{bmatrix}E_{ds}(t_i)\\ E_{qs}(t_i)\end{bmatrix} \quad (6)$$

A cost function is chosen such that

$$\begin{aligned}J[\boldsymbol{x}(t_i)] = &\sum_{j=0}^{i}\lambda^{i-j}\Big(\boldsymbol{y}(t_j) - \boldsymbol{H}(t_j)\boldsymbol{x}(t_i)\Big)^T\\ &\times\Big(\boldsymbol{y}(t_j) - \boldsymbol{H}(t_j)\boldsymbol{x}(t_j)\Big)\end{aligned} \quad (7)$$

where $\lambda \in (0, 1)$ is the forgetting factor. The solution $\hat{\boldsymbol{x}}(t_i)$ that minimises the cost function $J[\boldsymbol{x}(t_i)]$ is obtained by the following least-squares algorithm such that [9]:

$$\hat{\boldsymbol{x}}(t_i) = \hat{\boldsymbol{x}}(t_{i-1}) + \boldsymbol{k}(t_i)[\boldsymbol{y}(t_i) - \boldsymbol{H}(t_i)\hat{\boldsymbol{x}}(t_{i-1})] \quad (8)$$

$$\boldsymbol{r}_e(t_i) = \lambda\boldsymbol{I} + \boldsymbol{H}(t_i)\boldsymbol{P}(t_{i-1})\boldsymbol{H}(t_i)^T \quad (9)$$

$$\boldsymbol{k}(t_i) = \boldsymbol{P}(t_{i-1})\boldsymbol{H}(t_i)^T\boldsymbol{r}_e(t_i)^{-1} \quad (10)$$

$$\begin{aligned}\boldsymbol{P}(t_i) = &\lambda^{-1}\boldsymbol{P}(t_{i-1}) - \lambda^{-1}\boldsymbol{P}(t_{i-1})\\ &\times\boldsymbol{H}(t_i)^T\boldsymbol{r}_e(t_i)^{-1}\boldsymbol{H}(t_i)\boldsymbol{P}(t_{i-1})\end{aligned} \quad (11)$$

where $\hat{\boldsymbol{x}}(t_0) = \boldsymbol{0}$, $\boldsymbol{P}(t_0) = \pi_0\boldsymbol{I} \in \mathbb{R}^{4\times4}$ and $\pi_0 > 0$ is the initial error covariance constant. From eqn. 8, the authors obtain

the phase angles of the positive-sequence voltage, such that

$$\hat{\phi}(t_i) = \tan^{-1}[\hat{E}^p_{qe}(t_i)/\hat{E}^p_{de}(t_i)] \quad (12)$$

Fig. 3 shows the flowchart of the proposed phase-angle estimation algorithm.

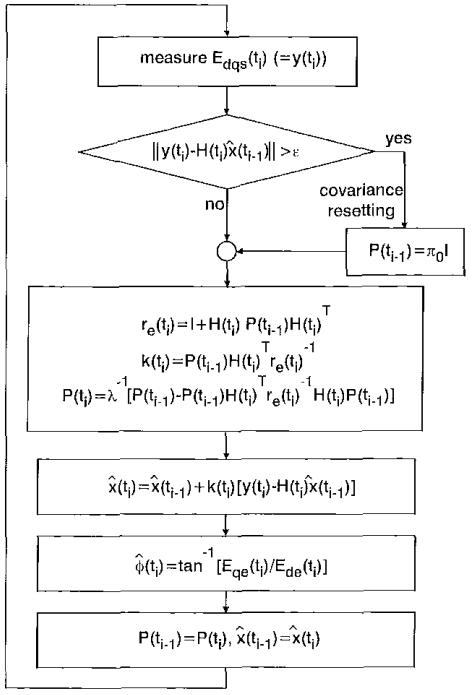

Fig. 3 *Flowchart of proposed phase-angle estimation algorithm*

To enhance the tracking speed of the phase-angle jump caused by sudden voltage sag and/or unbalance, the authors have used the covariance resetting technique. The existence of a phase-angle jump is discerned from the normal condition by the estimation error magnitude. Hence, if the estimation error is larger than a given boundary value ε, i.e. $\|\boldsymbol{y}(t_i) - \boldsymbol{H}(t_i)\hat{\boldsymbol{x}}(t_{i-1})\| > \varepsilon$, then $\boldsymbol{P}(t_{i-1})$ is reset with the initial error covariance $\pi_0\boldsymbol{I}$. To avoid frequent resetting caused by noise under the normal condition, the boundary value ε does not need to be very small. A heuristic guideline is to set ε equal to 20~40% of the peak amplitude of the nominal source voltage. Note also that, with the WLSE, noise immunity of the estimator can be increased by selecting a larger forgetting factor λ.

Table 1: Calculation time of the proposed WLSE algorithm with a DSP TMS320C31

Calculation contents	Number of instructions	Time, μs
$\boldsymbol{P}(t_{i-1})\boldsymbol{H}(t_i)^T$	32	1.056
$\boldsymbol{r}_e(t_i) = \boldsymbol{I} + \boldsymbol{H}(t_i)\boldsymbol{P}(t_{i-1})\boldsymbol{H}(t_i)^T$	36	1.188
$\boldsymbol{k}(t_i) = \boldsymbol{P}(t_{i-1})\boldsymbol{H}(t_i)^T\boldsymbol{r}_e(t_i)^{-1}$	47	1.551
$\boldsymbol{P}(t_i) = \lambda^{-1}[\boldsymbol{P}(t_{i-1}) - \boldsymbol{P}(t_{i-1})\boldsymbol{H}(t_i)^T\boldsymbol{r}_e(t_i)^{-1}\boldsymbol{H}(t_i)\boldsymbol{P}(t_{i-1})]$	104	3.432
$\hat{\boldsymbol{x}}(t_i) = \boldsymbol{k}(t_i)[\boldsymbol{y}(t_i) - \boldsymbol{H}(t_i)\hat{\boldsymbol{x}}(t_{i-1})]$	20	0.660
$\tan^{-1}$ (look-up table)	25	0.825
Total	264	8.712

3.2 Computation time of the WLSE algorithm

The proposed WLSE algorithm does not require much calculation effort, because it is based on the recursive least-squares algorithm. For example, if a DSP TMS320C31 is used with an instruction time of 33ns, the calculation time is about 10μs (300 instruction cycles) as shown in Table 1. Considering a 5kHz switching frequency, the PWM period is equal to 200μs. Hence, 10μs calculation time lies within a tolerable range in practical implementation.

3.3 Frequency update algorithm

In the previous phase-angle estimation algorithm, the frequency information is quite important. If the frequency ω used in eqns. 1 and 3 is erroneous, then it will lose synchronism yielding oscillating phase-angle error. Hence, to accommodate the variable frequency, the frequency estimate needs to be updated online. The authors denote by $\hat{\omega}$ an estimate of the source frequency ω. However, if $\hat{\omega} \neq \omega$, then $\hat{\phi}$ is no longer constant, but varies according to

$$\hat{\phi}(t_i) = \Delta\omega\tau + \hat{\phi}(t_{i-1}) \quad (13)$$

where $\Delta\omega = \omega - \hat{\omega}$ and $\tau = t_i - t_{i-1}$. Hence, the necessary condition for $\Delta\hat{\phi} \equiv \hat{\phi}(t_i) - \hat{\phi}(t_{i-1}) = 0$ is that $\Delta\omega = 0$, i.e. $\hat{\omega} = \omega$.

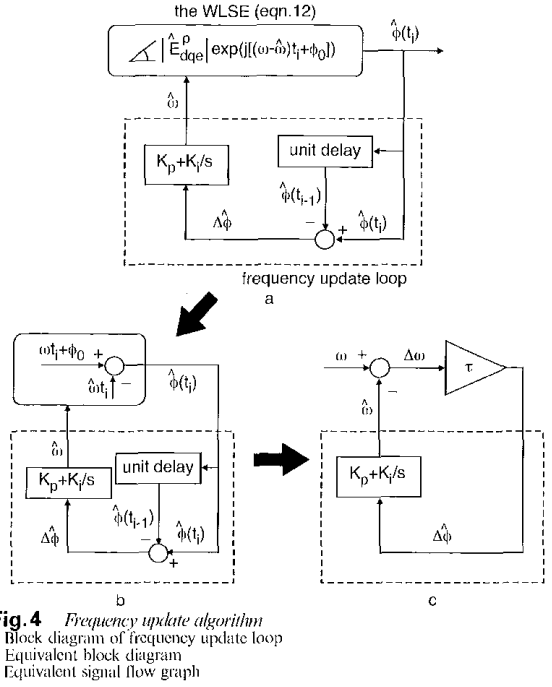

Fig. 4 *Frequency update algorithm*
a Block diagram of frequency update loop
b Equivalent block diagram
c Equivalent signal flow graph

On the other hand, if $\Delta\hat{\phi} \neq 0$, it implies $\Delta\omega \neq 0$. Hence, $\Delta\hat{\phi}$ can be utilised to enable $\hat{\omega}$ to track ω. As shown in Fig. 4, the basic idea for updating $\hat{\omega}$ is to employ a PI regulator such that $\Delta\hat{\phi}$ is regulated to a zero value. Then, the authors claim that the output of the PI regulator can be used for $\hat{\omega}$. Note that $\hat{\omega}$ is utilised for eqn. 4 along the WLSE algorithm. Fig. 4*a* shows the block diagram of the frequency update loop consisting of a PI regulator and a unit delay. Figs. 4*b* and *c* show the equivalent block diagram of the frequency update loop, and its equivalent signal flow diagram, respectively. Note that ϕ_0 is an initial phase angle. From Fig. 4*c*, the transfer function $\hat{\omega}/\omega$ is

$$\frac{\hat{\omega}}{\omega} = \frac{\tau(K_p + K_i/s)}{1 + \tau(K_p + K_i/s)} = \frac{s\tau K_p + \tau K_i}{s(1 + \tau K_p) + \tau K_i} \quad (14)$$

Application of the final value theorem to $\Delta\omega$, for a step change in ω, gives

$$\lim_{t\to\infty} \Delta\omega = \lim_{s\to 0} s(\omega - \hat{\omega})$$
$$= \lim_{s\to 0} s\frac{1}{s}\left(1 - \frac{s\tau K_p + \tau K_i}{s(1 + \tau K_p) + \tau K_i}\right) = 0 \quad (15)$$

It can be seen from eqn. 15 that $\hat{\omega}$ tracks the real value ω without an offset error. To avoid a possible instability of the WLSE algorithm, the PI gain of this frequency update algorithm must not be large.

4 Simulation and experimental results

4.1 Phase angle estimation

The authors performed simulation and experiments with the example source voltage containing 20% 5th- (300Hz), 5% 7th- (420Hz), and 3% 11th- (660Hz) order harmonics that were used in [10]:

$$\begin{bmatrix} E_a \\ E_b \\ E_c \end{bmatrix} = \begin{bmatrix} 60\cos(\omega t) \\ 60\cos(\omega t-120°) \\ 60\cos(\omega t+120°) \end{bmatrix} + \begin{bmatrix} 12\cos(5\omega t) \\ 12\cos(5(\omega t-120°)) \\ 12\cos(5(\omega t+120°)) \end{bmatrix} + \begin{bmatrix} 3\cos(7\omega t) \\ 3\cos(7(\omega t-120°)) \\ 3\cos(7(\omega t+120°)) \end{bmatrix} + \begin{bmatrix} 2\cos(11\omega t) \\ 2\cos(11(\omega t-120°)) \\ 2\cos(11(\omega t+120°)) \end{bmatrix} \quad (16)$$

Then the resulting total harmonic distortion (THD) is equal to 20.8%. Total harmonic distortion (THD) of the utility voltage is typically less than 5%. However, in the industrial site, it is higher than 5% due to various nonlinear loads [2].

After 250ms, the authors make the source voltage experience further abrupt voltage sag in the a and b phases and voltage swell in the c phase in a step manner, such that

$$\begin{bmatrix} E_a \\ E_b \\ E_c \end{bmatrix} = \begin{bmatrix} 59\cos(\omega t+31°) \\ 33\cos(\omega t-63°) \\ 66\cos(\omega t+181°) \end{bmatrix} + \begin{bmatrix} 12\cos(5\omega t) \\ 12\cos(5(\omega t-120°)) \\ 12\cos(5(\omega t+120°)) \end{bmatrix} + \begin{bmatrix} 3\cos(7\omega t) \\ 3\cos(7(\omega t-120°)) \\ 3\cos(7(\omega t+120°)) \end{bmatrix} + \begin{bmatrix} 2\cos(11\omega t) \\ 2\cos(11(\omega t-120°)) \\ 2\cos(11(\omega t+120°)) \end{bmatrix} \quad (17)$$

Then, the example voltage has about 35% unbalance according to the definition of percentage unbalance in [5], and about 50° phase-angle jump. Figs. 5*a* and *b* depict the example waveform of $\{E_a, E_b, E_c\}$ and the corresponding synchronous d- and q-axis voltages $\{E_{de}, E_{qe}\}$, respectively. Fig. 5*c* shows the frequency spectrum of E_a, which indicates the existence of the harmonics. Note from Fig. 5*b* that the 2nd-order harmonics take place after t = 250ms, due to the negative sequence caused by the unbalance.

Fig. 6 shows the simulation results of $\hat{\phi}$ and $\{\hat{E}^p_{de}, \hat{E}^p_{qe}\}$ with the proposed estimation scheme for $\{\lambda, \pi_0\}$ = {0.99, 50} and {0.99, 10}. With the proposed estimation scheme, the estimated value $\hat{\phi}$ tracks the step change well, even in the presence of such an intensive harmonic disturbance. Note that increasing π_0 has the effect of increasing the convergence gain, while increasing λ enhances the averaging effects, as is well known in the analysis of the least-squares method.

For the experiments, the control board was made with the DSP TMS320C31 with the sampling (or feedback) frequency of 3kHz, ε = 18 and $\{\lambda, \pi_0\}$ = {0.99, 50}, {0.99, 10}. The unbalanced voltage sag was generated by a programmable AC power supply. Fig. 7 shows the experimental results of $\hat{\phi}$ and $\{\hat{E}^p_{de}, \hat{E}^p_{qe}\}$ with the proposed estimation scheme under the same condition as in the simulation. The experimental results shown in Fig. 7 look quite similar to the simulation results shown in Fig. 6.

Fig. 8 also shows experimental results of $\hat{\phi}$ and $\{\hat{E}^p_{de}, \hat{E}^p_{qe}\}$ under the same condition, except that a harmonic disturbance is excluded. Comparing it with Fig. 7, it is noticed that the transient period becomes shorter. The estimated phase angle $\hat{\phi}$ tracks the step change in about 800μs (2~3 steps) for π_0 = 50 and 1.6ms (5 steps) for π_0 = 10.

4.2 Frequency updating

The authors have also demonstrated the performance of the frequency update algorithm through simulation and experiment. In the simulation, the source frequency $\omega/2\pi$ was changed gradually from 60 to 50Hz, and then back to 60Hz. The authors set the PI gains such that K_p = 0.0004 and K_i = 0.00005. Figs. 9*a* and *b* show the simulation results of the frequency estimate $\hat{\omega}/2\pi$ and the estimation

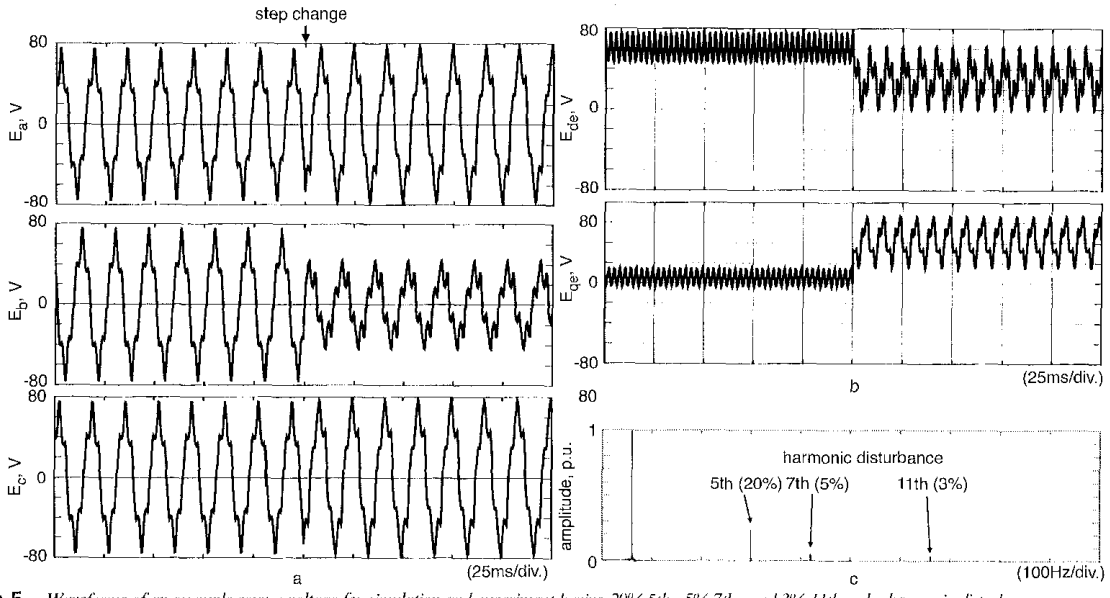

Fig. 5 *Waveforms of an example source voltage for simulation and experiment having 20% 5th-, 5% 7th-, and 3% 11th-order harmonic disturbances*
After 250ms, voltage sag (a, b phases) and swell (c phase) take place in a step manner
a $\{E_a, E_b, E_c\}$
b Corresponding synchronous d- and q-axis voltages $\{E_{de}, E_{qe}\}$
c Frequency spectrum of E_a

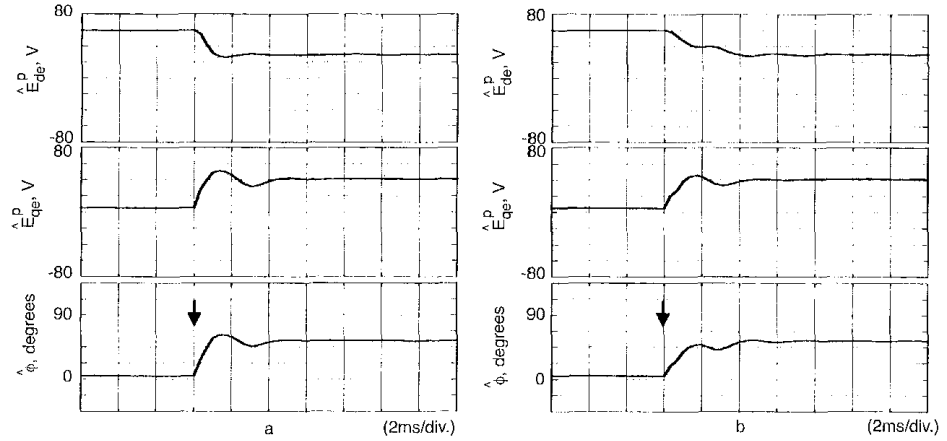

Fig. 6 *Simulation results of proposed estimation scheme with source voltage shown in Fig. 5*
$\{\lambda, \pi_0\} = (a)\ \{0.99, 50\}, (b)\ \{0.99, 10\}$

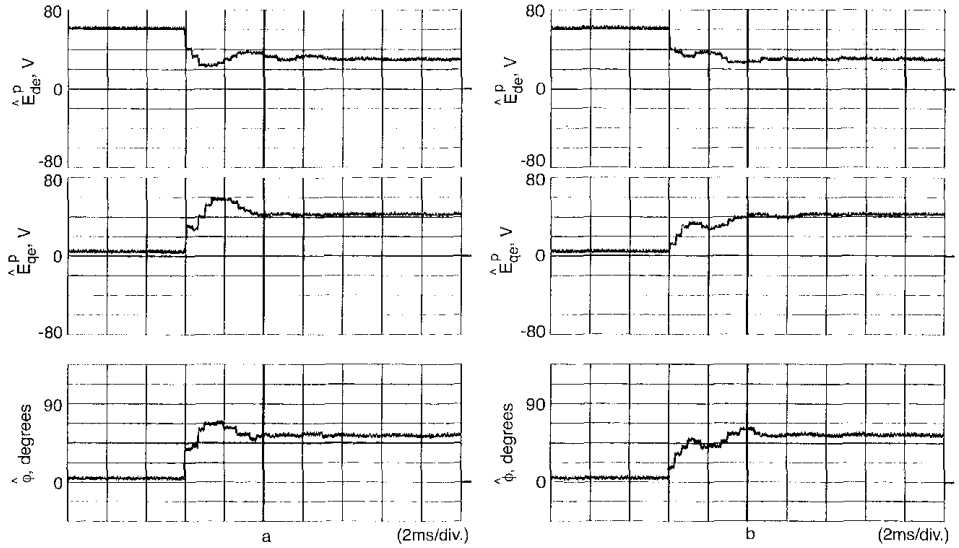

Fig. 7 *Experimental results of proposed estimation scheme with source voltage shown in Fig. 5*
$\{\lambda, \pi_0\} = (a)\ \{0.99, 50\}, (b)\ \{0.99, 10\}$

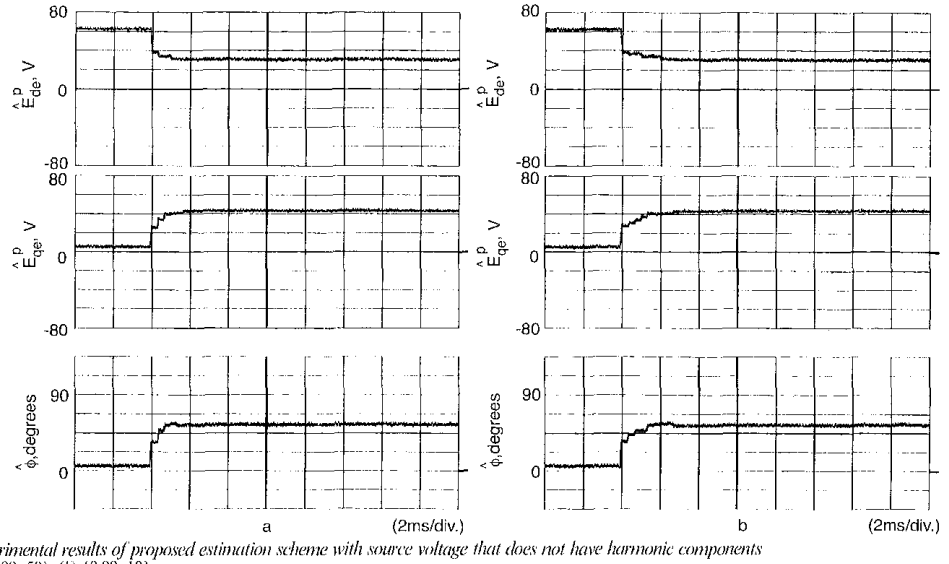

Fig. 8 *Experimental results of proposed estimation scheme with source voltage that does not have harmonic components*
$\{\lambda, \pi_0\} = (a)\ \{0.99, 50\}, (b)\ \{0.99, 10\}$

error $(\omega - \hat{\omega})/2\pi$, respectively. It can be clearly seen from Fig. 9 that the varying frequency is estimated well with the proposed frequency update algorithm.

In the experiment, the authors were not able to change the source frequency. Thus, a 60Hz balanced voltage source has been used with the same PI gain. However, the

initial frequency estimate 50Hz is considered, i.e. $\omega/2\pi$ = 60Hz, $\hat{\omega}(t_0)/2\pi$ = 50Hz. Figs. 10*a* and *b* show the experimental result of the frequency error $(\omega - \hat{\omega})/2\pi$, and the voltage estimation error $E_a - \hat{E}_a$, respectively. It can be seen from Fig. 10 that the initial 10Hz error vanishes in about 30s.

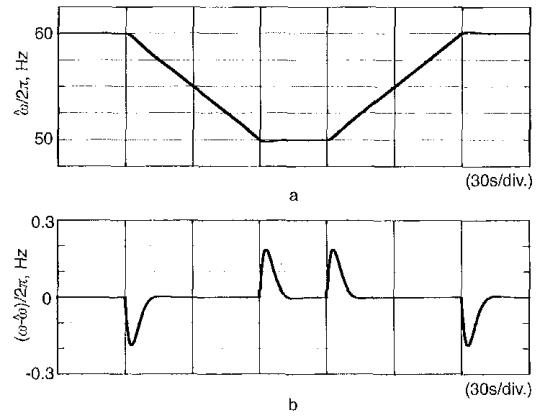

Fig. 9 *Simulation results of frequency update algorithm when frequency changes*
a Frequency estimate $\hat{\omega}/2\pi$
b Frequency estimation error $(\omega - \hat{\omega})/2\pi$

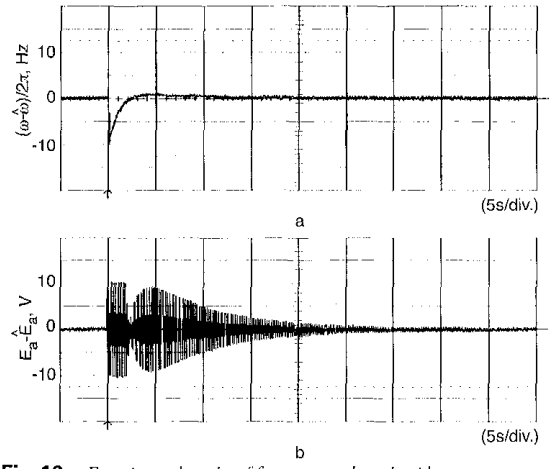

Fig. 10 *Experimental results of frequency update algorithm*
a Frequency estimation error $(\omega - \hat{\omega})/2\pi$ for an initial wrong estimate $\hat{\omega}(t_0) = 2\pi \times 50$, $(\omega = 2\pi \times 60)$
b Corresponding voltage estimation error $E_a - \hat{E}_a$

5 Concluding remarks

The authors have proposed a phase-angle estimation algorithm that acted promptly when a sudden voltage sag and/or unbalance took place. The proposed algorithm was derived from the weighted least-squares estimation method with the covariance resetting technique. It has enabled the authors to measure, instantaneously, both the positive and the negative sequences separately. In many applications, the estimated phase-angle of the positive sequence is used for setting the reference frame, and the estimated negative-sequence component is used for unbalance compensation. The proposed method can be differentiated from the conventional filter techniques by the fast transient response. With the frequency update algorithm, the time-varying frequency can be also estimated. Hence, the proposed phase-angle estimation scheme is thought to be suitable to UPS, active filters, or voltage compensators in which the fast response is essential. This paper provides an example application in the Appendix (Section 7). Technically, the authors can increase the immunity to noise by choosing a larger λ. Faster convergence can be achieved by choosing the larger π_0. According to simulation study, recommended parameters are $\lambda \in [0.9, 1)$ and $\pi_0 \in [10, 1000]$. This paper has demonstrated the superior performance through computer simulations as well as through experiments.

6 References

1 MELHORN, C.J., DAVIS, T.D., and BEAM, G.E.: 'Voltage sags: Their impact on the utility and industrial customers', *IEEE Trans. Ind. Appl.*, 1998, **IA-34**, (3), pp. 549–558
2 YALCINKAYA, G., BOLLEN, M.H.J., and CROSSLEY, P.A.: 'Characterization of voltage sags in industrial distribution systems', *IEEE Trans. Ind. Appl.*, 1998, **IA-34**, (4), pp. 682–688
3 BEEMAN, D.: 'Industrial power system handbook' (McGraw-Hill, 1955)
4 ENJETI, P.N., and CHOUDHURY, S.A.: 'A new control strategy to improve the performance of a PWM AC to DC converter under unbalanced operating conditions', *IEEE Trans. Power Electron.*, 1993, **PE-8**, (4), pp. 493–500
5 HOCHGRAF, C., and LASSETER, R.H.: 'Statcom controls for operation with unbalanced voltages', *IEEE Trans. Power Deliv.*, 1998, **PWRD-13**, (2), pp. 538–544
6 SIDHU, T.S., and SACHDEV, M.S.: 'An iterative technique for fast and accurate measurement of power system frequency', *IEEE Trans. Power Deliv.*, 1998, **PWRD-13**, (1), pp. 109–115
7 SONG, H.-S., and NAM, K.: 'Dual current control scheme for PWM converter under unbalanced input voltage conditions', *IEEE Trans. Ind. Electron.*, 1999, **IE-46**, (5), pp. 953–959
8 KIM, H.-S., MOK, H.-S., CHOE, G.-H., HYUN, D.-S., and CHOE, S.-Y.: 'Design of current controller for 3-phase PWM converter with unbalanced input voltage'. Proceedings of IEEE-PESC Annual Meeting, 1998, pp. 503–509
9 SÖDERSTRÖM, T., and STOICA, P.: 'System identification' (Prentice Hall, 1989)
10 GIRGIS, A.A., CHANG, W.B., and MAKRAM, E.B.: 'A digital recursive measurement scheme for on-line tracking of power system harmonics', *IEEE Trans. Power Deliv.*, 1991, **PWRD-6**, (3), pp. 1153–1160

7 Appendix: Example application – series voltage compensator

Fig. 11 shows the structure of a series voltage compensator which compensates for instantaneous voltage sag. If a voltage sag takes place in one or two phases of a three-phase power source, it will not only reduce the RMS level, but also cause a jump in the phase angle, and generate a negative-sequence voltage [2].

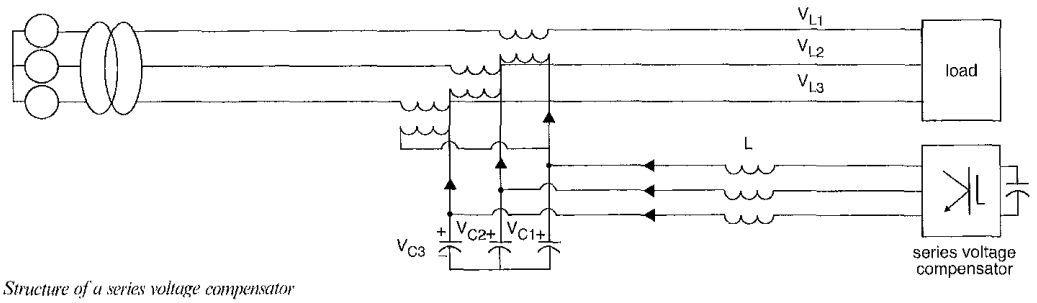

Fig. 11 *Structure of a series voltage compensator*

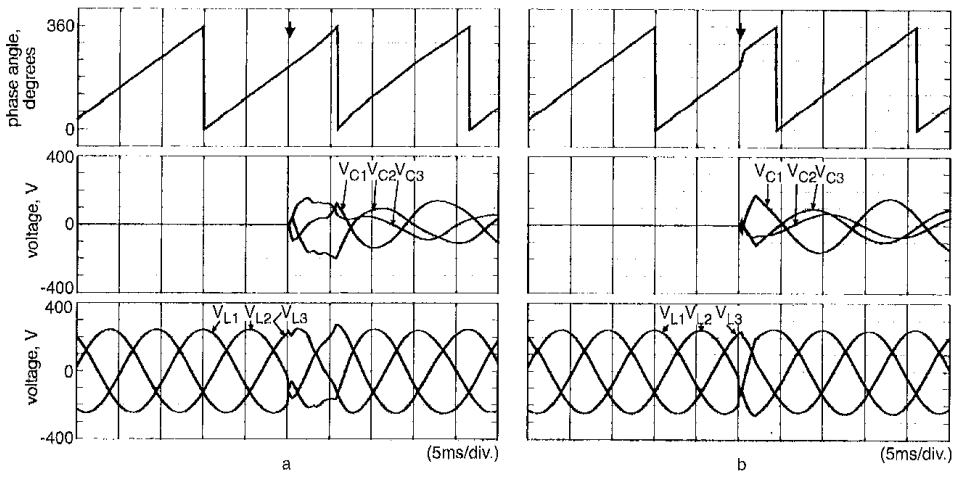

Fig. 12 *Simulation results when a voltage sag takes place in b-phase*
a With conventional phase-angle detection method that utilises PLL
b With proposed estimation algorithm

Fig. 12*a* shows the performance of the voltage compensator when a conventional phase-angle estimation method is used with phase-locked loop (PLL). Fig. 12*b* shows the performance with the proposed phase-angle estimation algorithm. Plots in the first row show the measured phase angle $\theta = \hat{\omega}t_i + \hat{\phi}(t_i)$, in the second row the compensation voltage (filter capacitor voltage) $\{V_{Ca}, V_{Ca}, V_{Ca}\}$, and in the third row the compensated load terminal voltage, $\{V_{La}, V_{Lb}, V_{Lc}\}$. A lowpass filter in the PLL generates a phase delay or phase-angle estimation error in the transient state. The phase-angle error results in an increase in the compensation voltage, often resulting in the saturation of the compensation voltage, as shown in Fig. 12*a*. However, with the proposed method, the authors can find the exact phase-angle of the source voltage, even when the source voltage changes abruptly. Hence, the authors can achieve the complete compensation even in the transient state and without additionally increasing the voltage or current rating, as shown in Fig 12*b*.